Motile Topological Defects Hinder Dynamical Arrest in Dense Liquids of Active Ellipsoids

Pragya Arora[,1] A. K. Sood,[2,3] and Rajesh Ganapathy[3,4]

[1]*Chemistry and Physics of Materials Unit, Jawaharlal Nehru Centre for Advanced Scientific Research,*
Jakkur, Bangalore - 560064, India
[2]*Department of Physics, Indian Institute of Science, Bangalore- 560012, India*
[3]*International Centre for Materials Science, Jawaharlal Nehru Centre for Advanced Scientific Research,*
Jakkur, Bangalore - 560064, India
[4]*School of Advanced Materials (SAMat), Jawaharlal Nehru Centre for Advanced Scientific Research,*
Jakkur, Bangalore - 560064, India

Recent numerical studies have identified the persistence time of active motion as a critical parameter governing glassy dynamics in dense active matter. Here we studied dynamics in liquids of granular active ellipsoids with tunable persistence and velocity. We show that increasing the persistence time at moderate supercooling is equivalent to increasing the strength of attraction in equilibrium liquids and results in reentrant dynamics not just in the translational degrees of freedom, as anticipated, but also in the orientational ones. However, at high densities, motile topological defects, unique to active liquids of elongated particles, hindered dynamical arrest. Most remarkably, for the highest activity, we observed intermittent dynamics due to the jamming-unjamming of these defects for the first time.

Physical intuition would suggest that making particles' in a supercooled liquid active, i.e., self-propelled, should shift the glass transition to higher densities or lower temperatures. Determining if this is indeed the case has been the mainstay of active glass research since experiments found that dynamics in confluent epithelial cell sheets shared remarkable similarities with equilibrium supercooled liquids and glasses [1]. The many subsequent numerical [2–6] and analytical studies [7–9] now anticipate that how the glass transition shifts depends explicitly on how the active forces are introduced [10], the form of the particle interactions, and crucially, the persistence time of particles' directed motion, τ_p [11]. In one class of well-studied active glass models, where the particle dynamics follow an Ornstein-Uhlenbeck stochastic process, the glass transition in active liquids of hard spheres shifts to higher densities with increasing τ_p [2]. For softer interactions, surprisingly, this shift is towards higher temperatures and lower densities because a large τ_p manifests as an effective swelling of the particles [6]. Since a finite persistence results in an activity-mediated effective attraction between even hard particles and leads to clustering [3,12], this model also anticipates reentrant liquid dynamics with τ_p for intermediate values of particle softness and even a reentrant glass transition [11]. This suggests a possible mapping with equilibrium "sticky" hard particle liquids where such a reentrant behavior is observed with increasing attraction strength [13–15]. Neither the increased tendency to glassify nor the reentrant dynamics have been seen in experiments largely because tuning τ_p systematically has not been

possible hitherto. Importantly, even while model details differ, studies anticipate that there is always a glass transition [16,17] and dynamical slowing down is accompanied by large collective swirls [2–9]. These swirls have indeed been observed in living active matter experiments [1,18,19].

Even though numerical or theoretical active glass studies take inspiration from findings in biological systems, where the constituents are anisotropic in shape, the models, barring the one on dumbbells [5], are for isotropic particle assemblies [11]. When alignment interactions are present, swirls are more pronounced [5], and furthermore, shape anisotropy invariably results in topological defects, which in active matter can be motile [20]. These defects play a crucial role in tissue morphogenesis, regeneration, and migration [21–23] although their role in glassy slowing down remains unexplored.

Here, we developed a system of active granular ellipsoids where τ_p and the particle velocity v can be tuned systematically while keeping the particle shape features fixed. Just like in the simulations of active Ornstein-Uhlenbeck particles (AOUPs) [9], the thermal noise is irrelevant here. We show that at mild to moderate supercooling the evolution of dynamics on increasing activity is akin to a system of hot adhesive particles with re-entrant dynamics in both the translational and orientational degrees of freedom (d.o.f.) A mode-coupling theory (MCT) inspired analysis reveals an increased tendency to glassify at the largest τ_p. Near the MCT glass transition and beyond, motile topological defects acted as conduits for structural

relaxation and suppressed glassy dynamics. Remarkably, at the largest τ_p, we observed intermittent jamming-unjamming events that are strikingly similar to that predicted to occur in so-called "extreme" active matter systems where τ_p is very large [24].

Our experimental system comprised of 3D-printed prolate ellipsoids (major axis $\alpha = 6$ mm and minor axes $\beta = 2.4$ mm, $\delta = 2.1$ mm) rendered active by vertical vibration. Earlier studies found that granules with an asymmetry in shape or mass, or friction coefficient μ, or some combination of these, under vertical agitation were polar active along the direction set by the asymmetry [25–28]. To tune activity, i.e., τ_p and/or v, the particle shape or size cannot be altered since this itself can strongly influence the nature of glassy dynamics. Instead, we designed particles with a fore-aft asymmetry in μ as well as mass. The former was brought about by exploiting a feature unique to the print process and the latter by introducing a hole along the particles' major axis (Supplemental Material S1, Fig. S1, and Fig. S2 [29]) [28]. Since changing the hole positions alters the particles' center of mass, we expected this to allow tuning activity.

Figure 1(a) shows snapshots of the ellipsoids for various hole positions and labeled a_1 through a_5. To further enhance the mass asymmetry, for a_5, one half of the ellipsoid was also made hollow during print (shaded region). The particles were placed on a horizontal plate that was coupled to an electromagnetic shaker through an air bearing and confined from above by a glass plate to enable imaging of dynamics [30]. The gap between plates Δ is such that $\delta < \Delta < \beta$ and particles cannot flip once confined. The drive frequency $f = 37$ Hz and amplitude $a = 1$ mm were kept constant, and the nondimensional acceleration $\Gamma = (4\pi^2 f^2 a/g) = 5.5$, where g is the acceleration due to gravity. For all activities, the particle motion was typical of run-and-tumble dynamics (movie S1 [29]), and as anticipated, both τ_p and v increased largely systematically (Supplemental Material S2, Fig. S3, and Table S1 [29]).

Armed with the capability to tune activity without changing the particle shape or size, we investigated the behavior of dense assemblies. For each activity, the projected particle area fraction ϕ was varied from 0.54 to ∼0.84. With increasing activity, we evidenced a clear and concomitant increase in the tendency for particles to form clusters [Fig. 1(b) for $\phi = 0.6$ and movies S2 and S3 [29], [3,12,31]]. This is quantitatively captured by the radial pair-correlation function $g(r)$, where the position of the first peak, which corresponds to the lateral alignment of the ellipsoids, remains fixed, while its height increases systematically with activity due to a higher likelihood of finding a nearby neighbor [Fig. 1(c) and inset]. Clearly, increasing activity has a role similar to increasing the strength of short-range attraction in equilibrium systems [2,3,11]. However, the clustering we observed was only
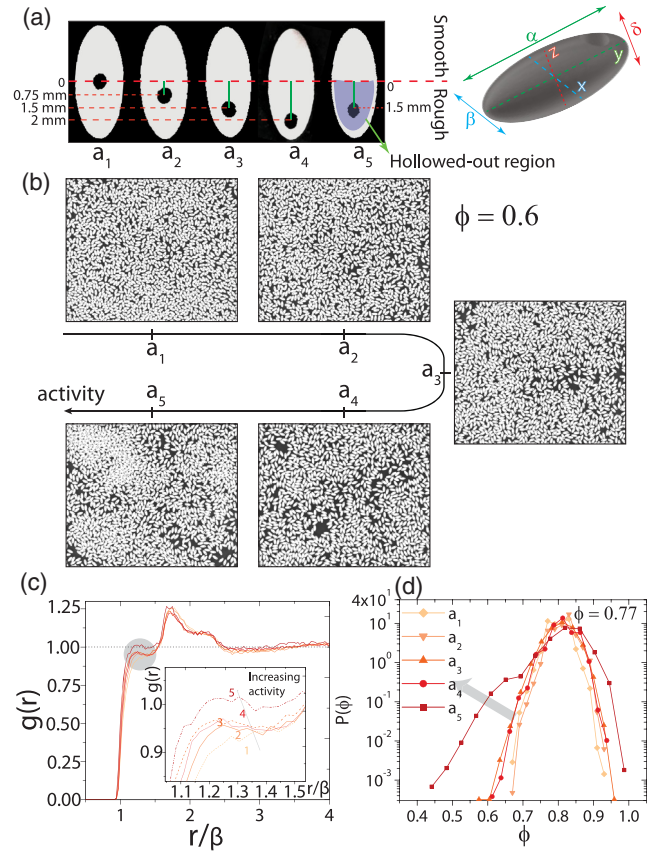

FIG. 1. (a) Left panel: Snapshots of the 3D-printed active ellipsoids. The central red dashed lines divide the rough portion of the particle from the smooth side. The hole position is progressively shifted across the major axis for a_1 to a_4. For a_5, one half of the ellipsoid is hollowed out and is shown by the blue shaded region. Right panel: 3D view of the ellipsoid showing its dimensions. (b) Snapshots of the experiment for $\phi = 0.6$ as a function of activity. Increasing the activity induces a strong tendency for particles to cluster. (c) Radial pair-correlation function, $g(r)$ at various activities. The inset shows the zoomed in region corresponding to the first peak of the $g(r)$. (d) The probability distribution of the coarse-grained density field $P(\phi)$ at various activities.

transient, indicating that this may not be motility-induced phase separation (MIPS) which manifests as a stable, dense macro droplet in a dilute gaslike background and is seen as a clear bimodal in the probability distribution of the coarse-grained density field $P(\phi)$ (see movie S4) [12]. While with increased activity $P(\phi)$ did develop a shoulder [Fig. 1(d)], its height is almost an order-of-magnitude smaller than the peak value of $P(\phi)$ (See Supplemental Material S4 and Figs. S4, S5 for other degrees of coarse graining [29]). Thus, unlike in isotropic active particle assemblies, MIPS is relatively weak here. Although surface roughness, like in our ellipsoids, can promote MIPS as it increases the particle collision time [32], our system did not show large-scale phase separation possibly due to the countereffect of the rodlike excluded volume torque [33].
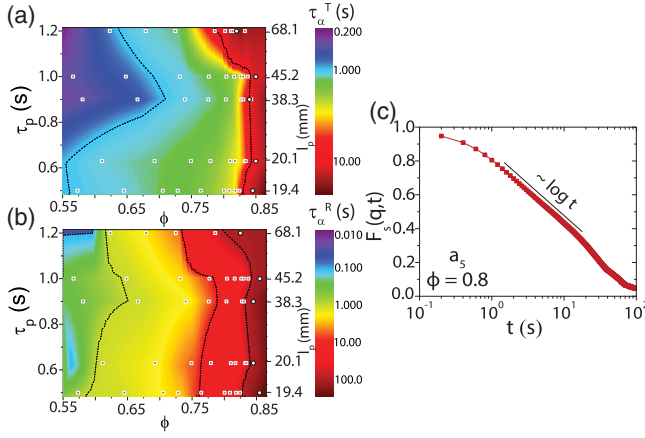
FIG. 2. [(a) and (b)] The relaxation dynamics phase diagram in the (τ_p, ϕ) plane for the translational and orientational d.o.f., respectively. The squares represent the τ_p and ϕ at which experiments were performed. In (a) and (b) the isochrones are shown by black dashed line. The color bar indicates the value of τ_α^T and τ_α^R. The τ_α values for ϕ's in between experimental data points were obtained from a linear interpolation. The second label on the y axis indicates the persistence length l_p. ϕ_g^T and ϕ_g^R, are shown by circles in (a) and (b), respectively. (c) $F_s(q = 1.4 \text{ mm}^{-1}, t)$ versus time for $\phi = 0.8$ for a_5.

Next, we interrogated how the activity-mediated effective attraction influenced dynamical slowing down. We quantified the relaxation dynamics of the system through the translational and orientational structural relaxation times τ_α^T and τ_α^R, respectively, obtained from the corresponding time correlators, these being the self-intermediate scattering function, $F_s(q,t)$, and the nth-order orientation correlation function, $L_n(t)$ (Supplemental Material S5 and Fig. S6 [29]). Figures 2(a) and 2(b) show the phase diagram of active ellipsoids in the (τ_p, ϕ) plane with the background colors representing the magnitude of τ_α^R and τ_α^T on a logarithmic scale. The second label on the y axis indicates the persistence length $l_p = v \tau_p$ (see Fig. S3 and Table S1 [29]). The gray squares represent the values of τ_p and ϕ at which experiments were performed and the isochrones are shown as black dashed lines. Consider a vertical cut at $\phi = 0.65$; increasing activity first speeds up relaxation and is then followed by a slowing down at the highest activities. This reentrant dynamics is a consequence of the competition between particle crowding and self-propulsion [2,3,11]. Initially, increasing τ_p leads to clustering of ellipsoids which opens up voids where self-propulsion dominates, resulting in a speeding up of dynamics. However, on further increasing activity (effective attraction), clustering dominates and slows down dynamics. This constitutes the first observation of reentrant dynamics in the liquid phase of active elongated particles.

A recently developed MCT for isotropic AOUPs predicts a nonmonotonic evolution of τ_α^T with τ_p [7,9]. Furthermore, a similar evolution of the glass transition with τ_p is also

expected in a small region of the parameter space [11]. There are, however, no such predictions for dense liquids of active ellipsoids as yet. Motivated by these studies, we fitted the relaxation times in the mild to moderate supercooled regime to power laws of the form $\tau_\alpha^{R,T} \propto (\phi_g^{R,T}/\phi - 1)^{-\gamma}$ and determined the orientational and translational glass transition area fractions, ϕ_g^R and ϕ_g^T, respectively. Here, γ is the scaling exponent (See Fig. S7 and Fig. S8 [29]). The black circles in Figs. 2(a) and 2(b) represent ϕ_g^T and ϕ_g^R, respectively. Although ϕ_g^T and ϕ_g^R shift to a smaller ϕ at the highest activity, we did not observe the stark reentrant behavior observed at moderate supercooling. Nevertheless, for a_5, $F_s(q, t)$ at $\phi = 0.8$ showed a logarithmic decay over more than a decade in t [Fig. 2(c)]. MCT first predicted such an anomalously slow relaxation for equilibrium sticky hard spheres near the A_3 singularity—the point where the attractive and repulsive glass transition lines meet [34]—and was later seen in many different passive liquids [15,35,36] but never in active ones. These observations suggest that the change in dynamics brought about by increasing activity mirrors the change due to an increase in the strength of interparticle attraction in equilibrium systems.

The above analysis revealed another correspondence between dense active and passive liquids of ellipsoids. For our active ellipsoids, which have an aspect ratio $p = (\alpha/\beta) = 2.5$, the ϕ_g^R and ϕ_g^T values are nearly same for each individual activity (Fig. S9 [29]). MCT for passive liquids of hard ellipsoids predicts orientational and translational glass transitions to occur at the same ϕ when $p \leq 2.5$, and orientational freezing to precede the translational one for $p > 2.5$ [15,37,38]. This correspondence with passive liquids is intriguing since a key ingredient of Ref. [6] is equal-time spatial velocity correlations, which should promote alignment interactions and aid slow down dynamics in the orientational d.o.f.

A close inspection of the particle dynamics did reveal swirls at moderate supercooling, and importantly, their macroscopic ordering was nematic, although our ellipsoids are polar active (Supplemental Material S8 and Fig. S10 [29]) [20,39]. We extracted the correlation length ζ of the swirls from the angle-averaged correlation function of the orientation of the displacement vectors of the active ellipsoids, $C(r) = \langle 2\cos^2 \Delta\theta(\mathbf{r}) - 1 \rangle$ (See Supplemental Material S9 and Fig. S11 [29]) [5]. Here, $\Delta\theta(\mathbf{r})$ is the angular separation between two displacement vectors separated by distance r, and the displacement was calculated over τ_α^T since our goal was only to determine how these swirls influenced structural relaxation. For $\phi < 0.78$, the regime that largely determines the ϕ_g values, and at all activities ζ remains small (Fig. S12 [29]). Thus, our active liquids behave like passive ones, and hence also the striking agreement with MCT predictions for the latter.

At deeper supercooling ($\phi > 0.79$), however ζ grew substantially and the swirls interfered with glassy slowing
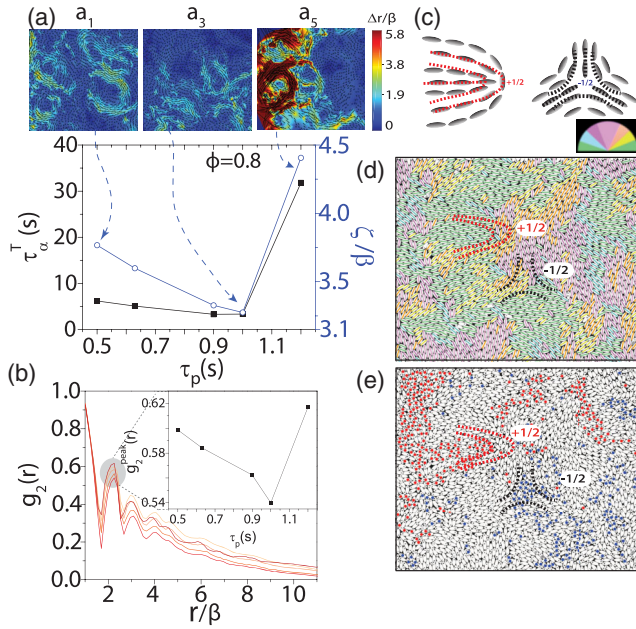
FIG. 3. (a) Translational relaxation time τ_α^T (black squares) and the normalized swirl correlation length ζ/β (blue circles) vs τ_p for $\phi = 0.8$. Particle displacement maps over τ_α^T for $\phi = 0.8$ for a_1, a_3, and a_5 corresponding to the data points shown by the dashed curved arrows. The color bar shows the magnitude of scaled particle displacement $\Delta r/\beta$ over τ_α^T. (b) Static orientational correlation function $g_2(r)$ vs r/β for various τ_p. Inset shows the height of the first peak of $g_2(r)$ as a function of τ_p. (c) Schematic of topological disclination defects of $\pm 1/2$ strength, respectively. (d) Orientational order field maps at $\phi = 0.8$. The red and black curved dashed lines depict the $+1/2$ and $-1/2$ disclination sites. We identified these defects by color-coding particle orientations as per the color wheel. (e) Top 20% translationally most mobile (red filled circles) and least mobile (blue-filled particles) at $\phi = 0.8$.

down. The top panels in Fig. 3(a) show the representative particle displacement maps, calculated over τ_α^T and color coded according to their magnitude for $\phi = 0.8$ (Movie S5 [29]). In dense liquids of passive ellipsoids with $p = 2.5$, the dynamics are essentially frozen at this ϕ [15]. Strikingly, ζ showed a clear nonmonotonicity with activity, mirroring the behavior of τ_α^T [Fig. 3(a) bottom panel]. To glean insights into the reentrant behavior, we calculated the static orientational correlation function $g_2(r)$ (Supplemental Material S9 [29]) at $\phi = 0.8$ [Fig. 3(b)]. At all r, $g_2(r)$ also showed clear reentrant behavior with τ_p [see inset to Fig. 3(b)]. For small and large values of τ_p, steric repulsion, and strong activity-mediate attraction, respectively, promote nematic alignment, while at intermediate activities, orientational disorder in the void spaces dominates and suppresses overall nematicity.

The nematic ordering of the swirls naturally led us to look for topological disclination defects of $\pm 1/2$ strength [40,41]. In active nematics, even sans momentum conservation [39,42], like our system, curvature-driven stresses

render $+1/2$ defects motile and $-1/2$ ones immotile [43]. The fingerprint of these defects in the orientational order field is shown in Figs. 3(c) and 3(d). As expected, only the $+1/2$ defects were motile, and this was the case for all the activities [see Supplemental Material S12, Fig. S13 [29]]. We, however, do not see measurable local density differences around $+1/2$ and $+1/2$ defect cores (See Supplemental Material S13, Fig. S14, and Table S2 [29]). More importantly, the top 20% translationally most-mobile (least-mobile) particles over the cage-breaking time t^*, obtained from the peak of the non-Gaussian parameter (Supplemental Material S14 and Fig. S15 [29]), were in the vicinity of $+1/2$ ($-1/2$) defects [Fig. 3(e) and Movie S6 in Ref. [29]]. Thus, these mobile topological defects act as conduits for structural relaxation and preclude the system from undergoing dynamical arrest at even high ϕ.

The influence of these mobile $+1/2$ defects on structural relaxation was most striking for a_5 since the active curvature stresses are largest here—the strong activity-mediated attraction also promotes strong nematic ordering of the ellipsoids. Here, we observed that both τ_α^T [Fig. 4(a)] and τ_α^R (Fig. S16 [29]) in fact saturated for $\phi > 0.8$. Furthermore, since our particles are rough, we observed the buildup and release of the active stresses manifest as jamming-unjamming events (Movie S7 [29]) [44]. We quantified these events through the coarse-grained displacement overlap function $d_\tau(t)$. To calculate this function, we binned the field of view into 30 square boxes of side 4.6α and then for each box and over τ_α^T, we calculated the average displacement, $\bar{d}_\tau(t)$, of the particles within the box. $d_\tau(t) = 1$ if $\bar{d}_\tau(t) > \alpha$ the particle size and zero otherwise. Figure 4(b) shows these jamming-unjamming events for $\phi = 0.8$ (top panel) and $\phi = 0.81$ (bottom panel). Figure 4(c) shows the dynamics of $+1/2$ defects in the jammed and unjammed regions. We found that the $+1/2$ defects were mobile in the unjammed region and almost stationary in the jammed region. Thus, these observations bring to the fore the crucial role of defects in glassy slowing down.

Collectively, our study shows that understanding glassy slowing down in generic dense active matter needs incorporating the rich physics of motile topological defects [20–22,41,42], unique to active liquids, with the well-developed concepts for classical liquids with sticky attraction [13–15,45,46]. A crucial experimental advance made here that allowed this inference was our strategy to tune the persistence time of the active particles. While at moderate supercooling, liquids of active ellipsoids behave like a 'hot' sticky classical liquid in both translational and orientational d.o.f., at deeper supercooling, this correspondence breaks even as motile $+1/2$ disclination defects inhibit glassy slowing down by providing a new pathway for structural relaxation. Remarkably, at the highest activity, our experiments revealed intermittent jamming-unjamming of these
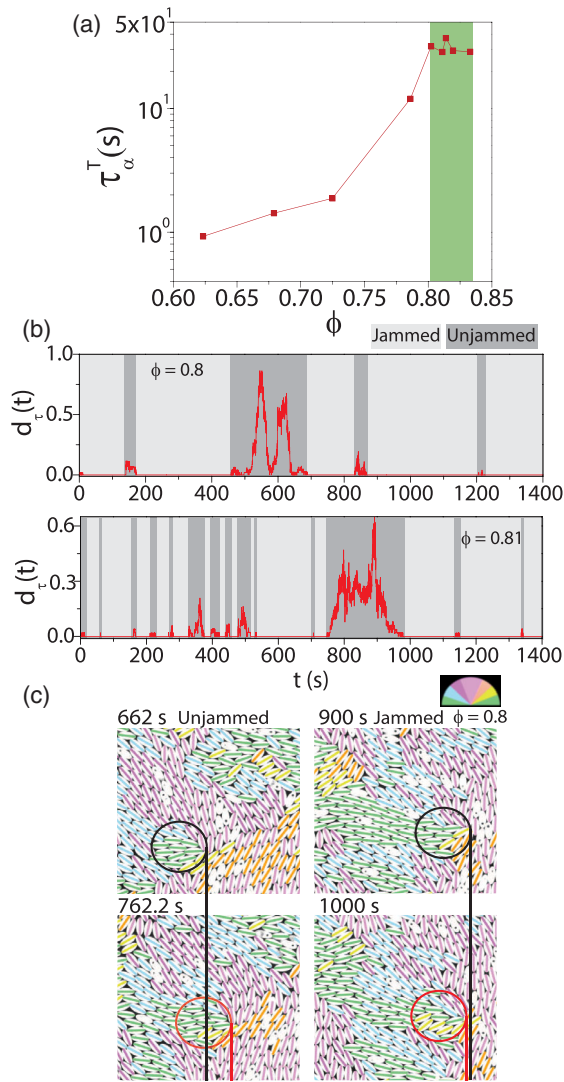
FIG. 4. (a) Translational relaxation times τ_α^T vs ϕ for a_5. Note the saturation in values of τ_α^T at large ϕ (green shaded region). (b) Displacement overlap function $d_\tau(t)$ for a_5 at $\phi = 0.80$ and $\phi = 0.81$. In the intermittent phase we see bursts of activity in the system, a characteristic of jamming-unjamming. (c) Orientational order field maps at $\phi = 0.80$. Dynamics of $+1/2$ defects in the jammed and unjammed regions over a duration of 100 s, respectively.

$+1/2$ disclinations. Although our experiments were restricted to particles with run-and-tumble dynamics, our approach to tune activity is far more generic. It should now be possible to explore the role of both particle shape and the nature of activity on active glass dynamics [28]. The future looks exciting now that well-controlled experiments with synthetic active matter can keep abreast with simulations [47].

---

[1] Thomas E. Angelini, Edouard Hannezo, Xavier Trepat, Manuel Marquez, Jeffrey J Fredberg, and David A. Weitz, Glass-like dynamics of collective cell migration, Proc. Natl. Acad. Sci. U.S.A. **108**, 4714 (2011).

[2] Ludovic Berthier, Nonequilibrium Glassy Dynamics of Self-Propelled Hard Disks, Phys. Rev. Lett. **112**, 220602 (2014).

[3] Demian Levis and Ludovic Berthier, Clustering and heterogeneous dynamics in a kinetic Monte Carlo model of self-propelled hard disks, Phys. Rev. E **89**, 062301 (2014).

[4] Ran Ni, Martien A. Cohen Stuart, and Marjolein Dijkstra, Pushing the glass transition towards random close packing using self-propelled hard spheres, Nat. Commun. **4**, 1 (2013).

[5] Rituparno Mandal, Pranab Jyoti Bhuyan, Pinaki Chaudhuri, Madan Rao, and Chandan Dasgupta, Glassy swirls of active dumbbells, Phys. Rev. E **96**, 042605 (2017).

[6] Elijah Flenner, Grzegorz Szamel, and Ludovic Berthier, The nonequilibrium glassy dynamics of self-propelled particles, Soft Matter **12**, 7136 (2016).

[7] Grzegorz Szamel, Elijah Flenner, and Ludovic Berthier, Glassy dynamics of athermal self-propelled particles: Computer simulations and a nonequilibrium microscopic theory, Phys. Rev. E **91**, 062304 (2015).

[8] Grzegorz Szamel, Theory for the dynamics of dense systems of athermal self-propelled particles, Phys. Rev. E **93**, 012603 (2016).

[9] Mengkai Feng and Zhonghuai Hou, Mode coupling theory for nonequilibrium glassy dynamics of thermal self-propelled particles, Soft Matter **13**, 4464 (2017).

[10] Saroj Kumar Nandi, Rituparno Mandal, Pranab Jyoti Bhuyan, Chandan Dasgupta, Madan Rao, and Nir S. Gov, A random first-order transition theory for an active glass, Proc. Natl. Acad. Sci. U.S.A. **115**, 7688 (2018).

[11] Ludovic Berthier, Elijah Flenner, and Grzegorz Szamel, How active forces influence nonequilibrium glass transitions, New J. Phys. **19**, 125006 (2017).

[12] Michael E. Cates and Julien Tailleur, Motility-induced phase separation, Annu. Rev. Condens. Matter Phys. **6**, 219 (2015).

[13] Khoa N. Pham, Antonio M. Puertas, Johan Bergenholtz, Stefan Ulrich Egelhaaf, A. Moussaïd, Peter N. Pusey, Andrew B. Schofield, Michael E. Cates, Matthias Fuchs, and Wilson C. K. Poon, Multiple glassy states in a simple model system, Science **296**, 104 (2002).

[14] Thomas Eckert and Eckhard Bartsch, Re-entrant Glass Transition in a Colloid-Polymer Mixture with Depletion Attractions, Phys. Rev. Lett. **89**, 125701 (2002).

[15] Chandan K. Mishra, Amritha Rangarajan, and Rajesh Ganapathy, Two-Step Glass Transition Induced by Attractive Interactions in Quasi-Two-Dimensional Suspensions of Ellipsoidal Particles, Phys. Rev. Lett. **110**, 188301 (2013).

[16] Ludovic Berthier and Jorge Kurchan, Non-equilibrium glass transitions in driven and active matter, Nat. Phys. **9**, 310 (2013).

[17] Alexander Liluashvili, Jonathan Ónody, and Thomas Voigtmann, Mode-coupling theory for active brownian particles, Phys. Rev. E **96**, 062608 (2017).

[18] Simon Garcia, Edouard Hannezo, Jens Elgeti, JeanFrançois Joanny, Pascal Silberzan, and Nir S. Gov, Physics of active jamming during collective cellular motion in a monolayer, Proc. Natl. Acad. Sci. U.S.A. **112**, 15314 (2015).

[19] Silke Henkes, Kaja Kostanjevec, J. Martin Collinson, Rastko Sknepnek, and Eric Bertin, Dense active matter model of motion patterns in confluent cell monolayers, Nat. Commun. **11**, 1405 (2020).

[20] Amin Doostmohammadi, Jordi Ignés-Mullol, Julia M. Yeomans, and Francesc Sagués, Active nematics, Nat. Commun. **9**, 3246 (2018).

[21] Thuan Beng Saw, Amin Doostmohammadi, Vincent Nier, Leyla Kocgozlu, Sumesh Thampi, Yusuke Toyama, Philippe Marcq, Chwee Teck Lim, Julia M. Yeomans, and Benoit Ladoux, Topological defects in epithelia govern cell death and extrusion, Nature (London) **544**, 212 (2017).

[22] Kyogo Kawaguchi, Ryoichiro Kageyama, and Masaki Sano, Topological defects control collective dynamics in neural progenitor cell cultures, Nature (London) **545**, 327 (2017).

[23] Linda S. Hirst and Guillaume Charras, Liquid crystals in living tissue, Nature (London) **544**, 164 (2017).

[24] Rituparno Mandal, Pranab Jyoti Bhuyan, Pinaki Chaudhuri, Chandan Dasgupta, and Madan Rao, Extreme active matter at high densities, Nat. Commun. **1**, 1 (2020).

[25] Arshad Kudrolli, Geoffroy Lumay, Dmitri Volfson, and Lev S. Tsimring, Swarming and Swirling in Self-Propelled Polar Granular Rods, Phys. Rev. Lett. **100**, 058001 (2008).

[26] Julien Deseigne, Olivier Dauchot, and Hugues Chaté, Collective Motion of Vibrated Polar Disks, Phys. Rev. Lett. **105**, 098001 (2010).

[27] Nitin Kumar, Harsh Soni, Sriram Ramaswamy, and A. K. Sood, Flocking at a distance in active granular matter, Nat. Commun. **5**, 1 (2014).

[28] Pragya Arora, A. K. Sood, and Rajesh Ganapathy, Emergent stereoselective interactions and self-recognition in polar chiral active ellipsoids, Sci. Adv. **7**, eabd0331 (2021).

[29] See Supplemental Material at http://link.aps.org/supplemental/10.1103/PhysRevLett.128.178002 for experimental details and supporting data.

[30] Daniel M. Harris and John W. M. Bush, Generating uniaxial vibration with an electrodynamic shaker and external air bearing, J. Sound Vib. **334**, 255 (2015).

[31] Yaouen Fily, Silke Henkes, and M. Cristina Marchetti, Freezing and phase separation of self-propelled disks, Soft Matter **10**, 2132 (2014).

[32] Sven Erik Ilse, Christian Holm, and Joost de Graaf, Surface roughness stabilizes the clustering of self-propelled triangles, J. Chem. Phys. **145**, 134904 (2016).

[33] Robin Van Damme, Jeroen Rodenburg, René Van Roij, and Marjolein Dijkstra, Interparticle torques suppress motility-induced phase separation for rodlike particles, J. Chem. Phys. **150**, 164501 (2019).

[34] K. Dawson, Giuseppe Foffi, Matthias Fuchs, Wolfgang Götze, Francesco Sciortino, Matthias Sperl, Piero Tartaglia, Th Voigtmann, and Emanuela Zaccarelli, Higher-order glass-transition singularities in colloidal systems with attractive interactions, Phys. Rev. E **63**, 011401 (2000).

[35] Sow-Hsin Chen, Wei-Ren Chen, and Francesco Mallamace, The glass-to-glass transition and its end point in a copolymer micellar system, Science **300**, 619 (2003).

[36] K. N. Pham, S. U. Egelhaaf, P. N. Pusey, and Wilson C. K. Poon, Glasses in hard spheres with short-range attraction, Phys. Rev. E **69**, 011503 (2004).

[37] M. Letz, R. Schilling, and A. Latz, Ideal glass transitions for hard ellipsoids, Phys. Rev. E **62**, 5173 (2000).

[38] Zhongyu Zheng, Feng Wang, Yilong Han, Glass Transitions in Quasi-Two-Dimensional Suspensions of Colloidal Ellipsoids, Phys. Rev. Lett. **107**, 065702 (2011).

[39] Robert Großmann, Igor S. Aranson, and Fernando Peruani, A particle-field approach bridges phase separation and collective motion in active matter, Nat. Commun. **11**, 5365 (2020).

[40] M. Cristina Marchetti, Jean-François Joanny, Sriram Ramaswamy, Tanniemola B. Liverpool, Jacques Prost, Madan Rao, and R. Aditi Simha, Hydrodynamics of soft active matter, Rev. Mod. Phys. **85**, 1143 (2013).

[41] Luca Giomi, Mark J. Bowick, Prashant Mishra, Rastko Sknepnek, and M. Cristina Marchetti, Defect dynamics in active nematics, Phil. Trans. R. Soc. A **372**, 20130365 (2014).

[42] Xia-qing Shi and Yu-qiang Ma, Topological structure dynamics revealing collective evolution in active nematics, Nat. Commun. **4**, 1 (2013).

[43] V. Narayan, S. Ramaswamy, and N. Menon, Long-lived giant number fluctuations in a swarming granular nematic, Science **317**, 105 (2007); O. J. Meacock, A. Doostmohammadi, K. R. Foster, J. M. Yeomans, and W. M. Durham, Bacteria solve the problem of crowding by moving slowly, Nat. Phys. **17**, 205 (2021).

[44] Anton Peshkov, Philippe Claudin, Eric Clément, and Bruno Andreotti, Active dry granular flows: Rheology and rigidity transitions, Europhys. Lett. **116**, 14001 (2016).

[45] Félix Ginot, Isaac Theurkauff, Demian Levis, Christophe Ybert, Lydéric Bocquet, Ludovic Berthier, and Cécile Cottin-Bizonne, Nonequilibrium Equation of State in Suspensions of Active Colloids, Phys. Rev. X **5**, 011004 (2015).

[46] Natsuda Klongvessa, Félix Ginot, Christophe Ybert, Cécile Cottin-Bizonne, and Mathieu Leocmach, Active Glass: Ergodicity Breaking Dramatically Affects Response to Self-Propulsion, Phys. Rev. Lett. **123**, 248004 (2019).

[47] Dapeng Bi, Xingbo Yang, M. Cristina Marchetti, and M. Lisa Manning, Motility-Driven Glass and Jamming Transitions in Biological Tissues, Phys. Rev. X **6**, 021011 (2016).

Correction: A missing source listing has been added to Ref. [43].